Charge density autocorrelation functions of molten salts: analytical treatment in the long-wavelength limit

2004 J. Phys.: Condens. Matter 16 L463

(http://iopscience.iop.org/0953-8984/16/41/L06)

INSTITUTE OF PHYSICS PUBLISHING JOURNAL OF PHYSICS: CONDENSED MATTER

J. Phys.: Condens. Matter **16** (2004) L463–L469 PII: S0953-8984(04)82906-0

LETTER TO THE EDITOR

Charge density autocorrelation functions of molten salts: analytical treatment in the long-wavelength limit

Taras Bryk and Ihor Mryglod

Institute for Condensed Matter Physics, National Academy of Sciences of Ukraine, 1 Svientsitskii Street, UA-79011 Lviv, Ukraine

Received 5 July 2004, in final form 26 August 2004
Published 1 October 2004
Online at stacks.iop.org/JPhysCM/16/L463
doi:10.1088/0953-8984/16/41/L06

Abstract

Nonhydrodynamic behaviour of charge density autocorrelation functions of molten salts is discussed. It is shown analytically within the three-variable generalized collective modes approach that kinetic propagating charge fluctuations make the contribution to the charge density autocorrelation functions nonvanishing in the long-wavelength limit. A comparison with molecular dynamics results is presented.

Microscopic dynamics of binary ionic liquids has for a long time been a focus of theoretical and computational studies because of the strong interplay of density and charge fluctuations. The strong Coulomb interaction is responsible for screening effects which appear in many specific features of molten salts while not being observable for non-ionic mixtures. Also, propagating charge excitations, often called optical-like modes, can be observed in charge–charge time correlation functions obtained in molecular dynamics (MD) simulations. For time correlation functions of binary ionic liquids, analytical results are known only in the hydrodynamic limit [1, 2]. The hydrodynamic set of dynamical variables in the case of a molten salt consists of four microscopic operators of total mass density $n_{\rm t}(k,t)$, charge density $n_q(k,t)$, longitudinal total mass current $J_{\rm t}^{\rm L}(k,t)$ and energy $e(k,t)$:

$$\mathbf{A}^{(\rm hyd)}(k,t) = \{n_{\rm t}(k,t), n_q(k,t), J_{\rm t}^{\rm L}(k,t), e(k,t)\}. \tag{1}$$

These four operators correspond to fluctuations of conserved quantities and describe the slowest dynamical processes in ionic melts. Indeed, charge current fluctuations reflect processes on shorter timescales than hydrodynamic ones—processes that cannot be taken into account correctly within the pure hydrodynamic picture. Therefore the only solution corresponding to propagating modes in the hydrodynamic regime is longitudinal sound waves. The hydrodynamic expression for charge–charge time correlation functions consists of two relaxation contributions, coming from charge conductivity and thermal diffusivity, and an oscillating symmetric contribution from sound excitations (the asymmetric contribution

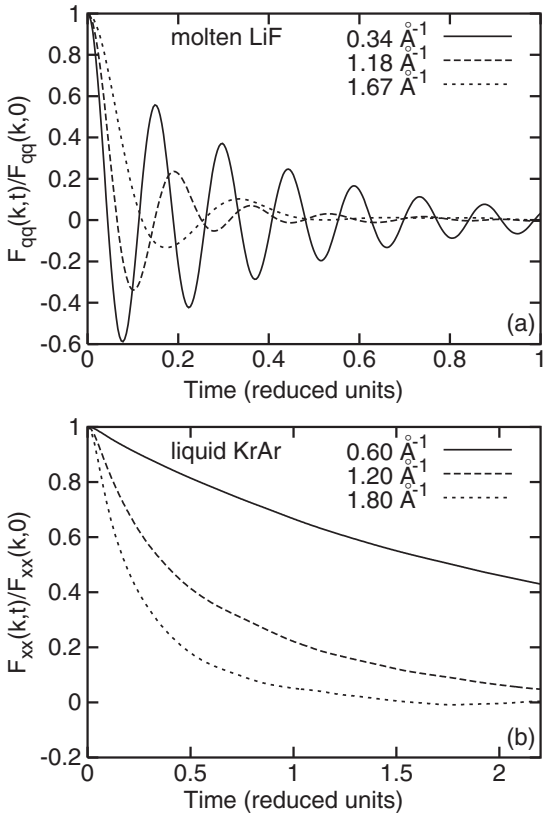

Figure 1. (a) Charge density autocorrelation functions for molten LiF at different wavenumbers. (b) The mass concentration time autocorrelation functions for a liquid Lennard-Jones mixture $F_{xx}(k,t)$. The timescales in the simulations of LiF and KrAr were $\tau_{\mathrm{LiF}} = 0.406$ ps and $\tau_{\mathrm{KrAr}} = 4.598$ ps, respectively.

corresponding to the non-Lorentzian shape of the dynamical structure factor $S_{qq}(k,\omega)$ is of order k^4) [2]:

$$F_{qq}(k,t)/F_{qq}(k,0) = A^{q}_{qq}(k)\mathrm{e}^{-d_q(k)t} + A^{\mathrm{th}}_{qq}(k)\mathrm{e}^{-d_{\mathrm{th}}(k)t} + B^{\mathrm{s}}_{qq}(k)\cos[c_{\mathrm{s}}kt]\mathrm{e}^{-\Gamma k^2 t}, \tag{2}$$

with $A^{q}_{qq}(k) = 1 - a_q k^2$, $A^{\mathrm{th}}_{qq}(k) = a_{\mathrm{th}}k^2$ and $B^{\mathrm{s}}_{qq}(k) = b_{\mathrm{s}}k^2$ being the amplitudes of the contributions from the charge conductivity, thermal diffusivity and sound excitations, respectively; c_{s} and Γ are the adiabatic speed of sound and sound attenuation coefficient. The mode amplitudes satisfy to the zeroth-order sum rule: $a_q = a_{\mathrm{th}} + b_{\mathrm{s}}$. As one may conclude from (2), the hydrodynamic expression implies that for sufficiently small wavenumbers, when $A^{q}_{qq}(k) \approx 1$, the shape of $F_{qq}(k,t)$ will be well described by a single-exponential function. However, the MD results for the charge density autocorrelation function $F_{qq}(k,t)$ disagree with the hydrodynamic expression (2). In figure 1(a) we show MD-derived charge–charge time correlation functions $F_{qq}(k,t)$ for molten LiF at 1287 K with three wavenumbers. The time correlation functions display strong oscillations with a tendency of increase of the frequency towards smaller wavenumbers that is completely opposite to the tendency usually observed for oscillations of the standard density–density time correlation functions due to sound propagation [3]. This means that the hydrodynamic expression (2) cannot be used for fitting to the MD data even in the long-wavelength region.

In contrast to the molten salts one, the autocorrelation function for mass concentration fluctuations, $F_{xx}(k,t)$, in liquid non-ionic mixtures can easily be fitted to a hydrodynamic two-exponential expression [3] in the region of small wavenumbers. In figure 1(b) the functions $F_{xx}(k,t)$ are shown for the case of the Lennard-Jones mixture KrAr at 116 K. At this thermodynamic point, for the Lennard-Jones liquid mixture we obtained in previous studies [4, 5] transverse and longitudinal propagating eigenmodes of optical phonon-like type. One can easily see the striking difference in behaviour between $F_{qq}(k,t)$ for molten salts and $F_{xx}(k,t)$ for liquid mixtures, although the dynamical variables of charge density $n_q(k,t)$ and mass concentration density $n_x(k,t)$ describe similar kinds of fluctuations and are proportional, via a constant [4]. Such a difference will be clarified here by means of the generalized collective modes (GCM) [6, 7] approach. Another of our tasks is formulating a simplified model for description of charge fluctuations and obtaining analytical expressions for mode contributions to $F_{qq}(k,t)$ in the long-wavelength limit.

Computer simulations for LiF at 1287 K were performed in the standard microcanonical ensemble on two model systems of 1000 and 500 particles in cubic boxes subject to periodic boundary conditions. Potentials in the Tosi–Fumi form for LiF were taken from [8]. The long-range interaction was treated by the Ewald method. Fifteen wavenumbers were sampled in MD simulations with the smallest value of $k_{\min} = 0.2711$ Å^{-1}. The main aim of the MD simulations was to obtain the time evolution of all hydrodynamic and short-time extended dynamical variables forming the basis set $\mathbf{A}^{(8)}(k,t)$ for the study of collective dynamics within the eight-variable GCM approach:

$$\mathbf{A}^{(8)}(k,t) = \{n_{\mathrm{t}}(k,t), n_q(k,t), J_{\mathrm{t}}^{\mathrm{L}}(k,t), J_q^{\mathrm{L}}(k,t), \varepsilon(k,t), j_{\mathrm{t}}^{\mathrm{L}}(k,t), j_q^{\mathrm{L}}(k,t), \dot{\varepsilon}(k,t)\}, \tag{3}$$

where the extended dynamical variables were represented by the time derivatives of the hydrodynamic variables. We estimated directly from MD the time correlation functions and relevant static averages needed for evaluation of matrix elements of the 8×8 matrices of the time correlation functions $\mathbf{F}(k,t)$ and their Laplace transforms $\tilde{\mathbf{F}}(k,z)$, and for calculation of GCM replicas of the relevant time correlation functions. Eigenvalues and eigenvectors of the generalized hydrodynamic matrix [7]

$$\mathbf{T}(k) = \mathbf{F}(k, t=0)\tilde{\mathbf{F}}^{-1}(k, z=0)$$

were calculated for each k-point sampled in molecular dynamics. Thus, in our approach there were no fitting or free parameters. The set of eigenvalues $z_\alpha(k)$ of the generalized hydrodynamic matrix $\mathbf{T}(k)$ formed the spectrum of collective excitations. Any MD-derived time correlation function of interest within the GCM approach has its GCM replica represented as a sum over the mode contributions:

$$F_{ij}^{(\mathrm{GCM})}(k,t) = \sum_{\alpha=1}^{8} G_{ij}^{\alpha}(k)\mathrm{e}^{-z_\alpha(k)t}, \tag{4}$$

where in general complex amplitudes $G_{ij}^{\alpha}(k)$ were estimated from the eigenvectors associated with the relevant eigenvalue $z_\alpha(k)$ [7, 9].

In figure 2 the imaginary parts of two complex eigenvalues $z_\alpha(k)$, which correspond to propagating excitations, are shown. Another branch of propagating excitations, corresponding to heat waves, was obtained in the region $k > 0.8$ Å^{-1}; however, we will focus in this study on the propagating density fluctuations. The dispersion curves in figure 2 shown by solid spline-interpolated lines were estimated from the eight-variable model (3). The physical origin of both branches can easily be established by a procedure proposed previously [4], which is based on an additional GCM study using separated subsets of dynamical variables, namely

$$\mathbf{A}^{(3i)}(k,t) = \{n_i(k,t), J_i^{\mathrm{L}}(k,t), j_i^{\mathrm{L}}(k,t)\}, \qquad i = t, q, \mathrm{Li}, \mathrm{F}. \tag{5}$$

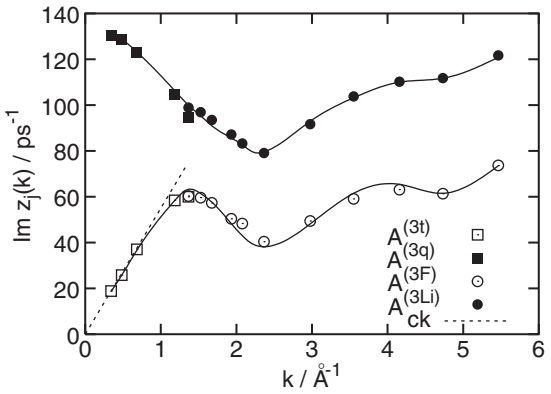

Figure 2. The dispersion of propagating collective excitations in molten LiF at 1287 K obtained in the eight-variable model $\mathbf{A}^{(8)}$ (spline-interpolated solid curves). Symbols show results obtained for separate sets of three dynamical variables. The dashed line shows the linear dispersion for sound excitations with $c = 5320$ m s^{-1}.

From figure 2 one can conclude that in the region $k < 1.4$ Å^{-1} the high-frequency branch is solely defined by propagating charge waves, while the low-frequency branch comes from the fluctuations of total density and in the long-wavelength region shows an almost linear dispersion law with the propagation speed $c = 5320$ m s^{-1}. In this region the low- and high-frequency branches correspond to acoustic and optical phonon-like excitations, respectively. Note that the frequency $\omega_{\mathrm{opt}}(k)$ is a decreasing function of wavenumber in the long-wavelength region in complete agreement with figure 1(a). For larger wavenumbers $k > 1.4$ Å^{-1} the 'partial' behaviour of both branches was established with low-and high-frequency branches describing solely heavy (F) and light (Li) subsystems in the melt. In figure 2 the symbols corresponding to the imaginary parts of complex eigenvalues obtained for four different separated three-variable subsets of dynamical variables are shown in regions of wavenumbers where the best correlation with the results of the eight-variable treatment was observed. This means that there are two domains in the k-space, where the behaviour of each branch of collective excitations can be well described in terms of 'intrinsic collective' $t-q$ dynamical variables in the small wavenumber region or 'partial' $A-B$ dynamical variables in the region of intermediate and large wavenumbers, because the $t-x$ (or $A-B$) cross-correlation between the dynamical variables in the corresponding domain of small (or large) wavenumbers is small.

The eight-variable approximation of the GCM approach allows us to reproduce fairly well the MD-derived time correlation functions of LiF. In figure 3 we show the quality of two GCM replicas for the smallest wavenumber charge density autocorrelation function, obtained with the basis sets $\mathbf{A}^{(8)}$ (dashed curve) and $\mathbf{A}^{(3q)}$ (dotted curve). The GCM replica obtained from the three-variable treatment of the charge subsystem (dotted curve) reproduces the oscillating behaviour of $F_{qq}(k, t)$, but contains oscillations that are less overdamped, because interaction between charge fluctuations and other hydrodynamic processes was not taken into account for the case of $\mathbf{A}^{(3q)}$. In the case of the eight-variable treatment, the quality of the GCM replica (dashed curve) is very good. Hence, the GCM approach, based on the hydrodynamic and more short-time variables, is able to reproduce the behaviour of the MD-derived function $F_{qq}(k, t)$, in contrast to the solely hydrodynamic treatment. Another advantage of the GCM approach is the possibility of separating mode contributions to the GCM replica according to (4). In order to make the mode contributions from (4) more suitable for analysis, we represented them in

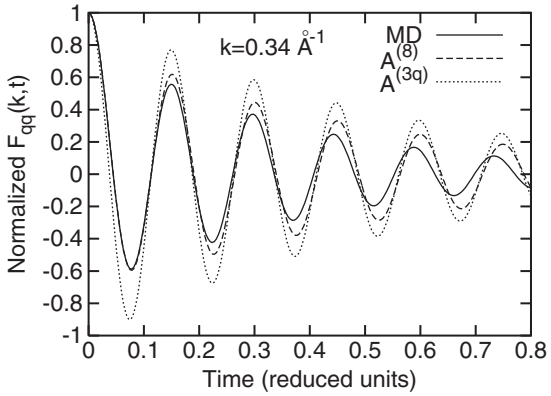

Figure 3. The charge density autocorrelation function for molten LiF obtained in MD simulations (solid curve) and its GCM replicas estimated from the eight-variable $\mathbf{A}^{(8)}$ (dashed curve) and three-variable $\mathbf{A}^{(3q)}$ (dotted curve) models.

the form of mode strengths of equation (2) [2, 4]:

$$F_{qq}^{(\mathrm{GCM})}(k,t)/F_{qq}(k,0) = \sum_{i}^{N_{\mathrm{rel}}} A_{qq}^{i}(k)\mathrm{e}^{-d_i(k)t} + \sum_{j}^{N_{\mathrm{pr}}}\{B_{qq}^{j}(k)\cos[\omega_j(k)t] + C_{qq}^{j}(k)\sin[\omega_j(k)t]\}\mathrm{e}^{-\Gamma_j(k)t}, \tag{6}$$

where in our case of eight eigenmodes for $k < 0.8$ Å^{-1} we had four ($N_{\mathrm{rel}} = 4$) relaxation modes $z_i(k) = d_i(k)$ and two pairs ($N_{\mathrm{pr}} = 2$) of propagating excitations $z_j(k) = \Gamma_j(k) \pm \mathrm{i}\omega_j(k)$. In figure 4 the mode amplitudes from the two main relaxation processes of electric conductivity $A_{qq}^{q}(k)$, the thermal diffusivity $A_{qq}^{\mathrm{th}}(k)$ and the two symmetric contributions coming from optical and acoustic branches of collective excitations are shown by symbol-connected lines for the case of eight-variable treatment of collective dynamics in molten LiF. In fact, equation (6) generalizes the hydrodynamic expression (2) to the case of additional nonhydrodynamic collective excitations in the liquid. From figure 4 it follows that for $k < 0.5$ Å^{-1} neither sound excitations nor the thermal diffusivity contribute to the charge–charge time correlation functions $F_{qq}(k,t)$; the shape of $F_{qq}(k,t)$ is determined solely by the relaxation process of the electric conductivity and propagating charge waves. Moreover, the contribution from the nonhydrodynamic charge waves is almost four times as large as that from the hydrodynamic relaxation process. This shows the striking difference between the molten salts with long-range interaction and non-ionic liquid mixtures for which the mode strength of optical-like excitations in $F_{xx}(k,t)$ vanishes rapidly towards small wavenumbers (see [5]).

A simple three-variable analytical approach within the GCM method can explain the behaviour of the mode strengths in figure 4. The 3×3 generalized hydrodynamic matrix $\mathbf{T}(k)$ constructed using the basis set of dynamical variables $\mathbf{A}^{(3q)}$ for the treatment of solely charge fluctuations in molten salts (5) has the same structure as was obtained in [5] for the case of mass concentration fluctuations in non-ionic solutions:

$$\mathbf{T}(k) = \begin{pmatrix} 0 & -\mathrm{i}k & 0 \\ 0 & 0 & -1 \\ -\mathrm{i}k^{-1}[\omega_{\mathrm{JJ}}^2 - \omega_{qq}^2]\tau_{qq}^{-1} & \omega_{\mathrm{JJ}}^2 & [\omega_{\mathrm{JJ}}^2(\omega_{qq}^2)^{-1} - 1]\tau_{qq}^{-1} \end{pmatrix}.$$

Note, however, that the input quantities, being expressed via the standard frequency moments of the charge–charge dynamical structure factors $\langle\omega_{qq}^n\rangle(k)$ [10], have, other than in liquid

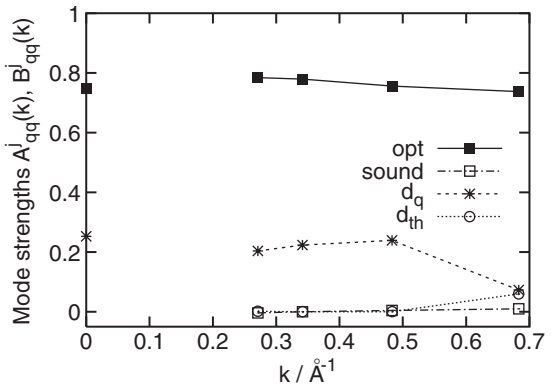

Figure 4. Mode amplitudes of different relaxation and propagation modes for the charge density autocorrelation functions obtained for molten LiF in the eight-variable GCM model $\mathbf{A}^{(8)}$ (symbols connected by lines). The filled box and asterisk at $k = 0$ correspond to mode amplitudes from propagating optical-like and charge relaxation excitations, respectively, as obtained from analytical expressions (10) and (11).

mixtures, asymptotics when $k \to 0$ due to the long-range interaction and electroneutrality condition:

$$\omega^2_{\mathrm{JJ}}(k) = \frac{\langle \dot{J}^{\mathrm{L}}_q(-k)\dot{J}^{\mathrm{L}}_q(k)\rangle}{\langle J^{\mathrm{L}}_q(-k)J^{\mathrm{L}}_q(k)\rangle}, \qquad \omega^2_{qq}(k) = \frac{k^2\langle J^{\mathrm{L}}_q(-k)J^{\mathrm{L}}_q(k)\rangle}{S_{qq}(k)},$$

$$\tau_{qq}(k) = \frac{1}{S_{qq}(k)}\int_0^\infty F_{qq}(k,t)\,\mathrm{d}t$$

tend to nonzero constants in the $k \to 0$ limit. Three eigenvalues of matrix $\mathbf{T}(k)$ in the long-wavelength limit are: a relaxation mode due to electric conductivity σ shifted by δ from its hydrodynamic value due to the interaction with propagation modes:

$$d_0 = \frac{4\pi\varepsilon}{\sigma} + \delta \equiv \frac{1}{\tau^0_{qq}} + \delta; \tag{7}$$

and a pair of complex-conjugate roots $\Gamma_0 \pm \mathrm{i}\omega_0$ corresponding to propagating charge waves with finite nonzero damping

$$\Gamma_0 = \frac{\omega^2_{\mathrm{JJ}}(0) - (2 + \delta\tau^0_{qq})\omega^2_{qq}(0)}{2\tau^0_{qq}\omega^2_{qq}(0)} \tag{8}$$

and frequency

$$\omega_0 = \sqrt{\frac{\omega^2_{\mathrm{JJ}}(0) - \omega^2_{qq}(0)}{1 + \delta\tau^0_{qq}} - \Gamma^2_0}. \tag{9}$$

Note that expressions (7)–(9) can be easily connected with the results derived for mass concentration collective excitations in non-ionic binary mixtures [5] by setting $\delta \to 0$, $\omega^2_{qq}(k) \sim k^2$, $\tau^0_{qq} \sim k^{-2}$.

An interesting conclusion can be drawn by comparison of the three-variable GCM results for the systems with long-range Coulomb interaction and non-ionic mixtures (or metallic liquids with screened Coulomb potentials): the mode contribution from optical-like excitations to the 'charge–charge' dynamical structure factor

$$S_{qq}(k,\omega) = S_{qq}(k)\left[A_{qq}\frac{d_k}{\omega^2 + d_k^2} + \frac{B_{qq}(k)\Gamma_k + C_{qq}(k)(\omega \pm \omega_k)}{(\omega \pm \omega_k)^2 + \Gamma_k^2}\right]$$

does not vanish in the limit $k \to 0$:

$$\lim_{k\to 0} A_{qq}(k) = 1 - \Delta + \mathrm{O}(k^2), \qquad \lim_{k\to 0} B_{qq}(k) = \Delta + \mathrm{O}(k^2) \tag{10}$$

with

$$\Delta = \frac{\omega_{qq}^2(0) + d_0^2 - 2d_0\Gamma_0}{(d_0 - \Gamma_0)^2 + \omega_0^2}. \tag{11}$$

In figure 4 we have shown at $k = 0$ the results for mode amplitudes of propagating charge waves (filled box) and the charge relaxation process (asterisk), which follow from our expressions (10) and (11) within the three-variable treatment of charge fluctuations using the basis set $\mathbf{A}^{(3q)}$. Good agreement between the three-variable analytical approach and the eight-variable numerical treatment supports our results. In the case of non-ionic mixtures or binary liquids with screened Coulomb interaction (metallic alloys) the real eigenvalue corresponding to concentration diffusion is a function of k^2 in the hydrodynamic region; hence the numerator in (11) vanishes as k^2 (see [5]), i.e. $\Delta \sim k^2$, and optical-like excitations in these systems are not visible in scattering experiments for small wavenumbers.

In summary, we have shown that the hydrodynamic expression [1, 2] for charge density autocorrelation functions cannot reproduce the shape of MD-derived functions. We solved a three-variable model for charge fluctuations analytically and obtained the contribution to $F_{qq}(k, t)$, nonvanishing in the limit $k \to 0$, coming from charge waves (optical phonon-like excitations) which, despite being nonhydrodynamic, nevertheless contribute to the charge density autocorrelation functions even in the long-wavelength limit. This feature is connected with the long-range Coulomb interaction in molten salts. Our calculations based on a generalized eight-variable treatment of the collective dynamics of molten LiF at 1287 K are in good agreement with the simplified three-variable analytical approach to charge fluctuations in molten salts.

References

[1] Giaquinta P V, Parrinello M and Tosi M P 1976 *Phys. Chem. Liq.* **5** 305
[2] March N H and Tosi M P 1984 *Coulomb Liquids* (London: Academic)
[3] March N H and Tosi M P 1976 *Atomic Dynamics in Liquids* (London: Macmillan)
[4] Bryk T and Mryglod I 2000 *J. Phys.: Condens. Matter* **12** 6063
[5] Bryk T and Mryglod I 2002 *J. Phys.: Condens. Matter* **14** L445
[6] de Schepper I M, Cohen E G D, Bruin C, van Rijs J C, Montfrooij W and de Graaf L A 1988 *Phys. Rev.* A **38** 271
[7] Mryglod I M, Omelyan I P and Tokarchuk M V 1995 *Mol. Phys.* **84** 235
[8] Ciccotti G, Jacucci G and McDonald I R 1976 *Phys. Rev.* A **13** 426
[9] Bryk T, Mryglod I and Kahl G 1997 *Phys. Rev.* E **56** 2903
[10] Hansen J-P and McDonald I R 1975 *Phys. Rev.* A **11** 2111